Lithuanian Journal of Physics, Vol. **58**, No. 2, pp. 188–193 (2018)
© Lietuvos mokslų akademija, 2018

DEVELOPMENT OF AlGaN/GaN/SiC HIGH-ELECTRON-MOBILITY TRANSISTORS FOR THz DETECTION

V. Jakštas [a], J. Jorudas [a], V. Janonis [a], L. Minkevičius [a], I. Kašalynas [a],

P. Prystawko [b], and M. Leszczynski [b]

[a] *Center for Physical Sciences and Technology, Saulėtekio 3, 10257 Vilnius, Lithuania*

[b] *Institute of High Pressure Physics UNIPRESS, Sokołowska 29/37, 01-142 Warsaw, Poland*

Email: vytautas.jakstas@ftmc.lt

Received 5 February 2018; revised 13 April 2018; accepted 21 June 2018

This paper reports on the AlGaN/GaN Schottky diodes (SDs) and high-electron-mobility transistors (HEMTs) grown on a semi-insulating SiC substrate. The electronic devices demonstrate an improved performance in comparison with the ones processed on a sapphire substrate. Both the SDs and HEMTs show much smaller leakage current density and a higher I_{ON}/I_{OFF} ratio, reaching values down to 3.0±1.2 mA/cm^2 and up to 70 dB under the reverse electric field of 340 kV/cm, respectively. The higher thermal conductivity of the SiC substrate leads to the increase of steady current and transconductance, and better thermal management of the HEMT devices. In addition, a successful detection of terahertz (THz) waves with the AlGaN/GaN HEMT is demonstrated at room temperature. These results open further routes for the optimization of THz designs which may result in development of novel plasmonic THz devices.

Keywords: SiC, GaN, Schottky diode, high electron mobility transistor, THz detection

PACS: 72.80.Ey, 07.57.Kp, 85.60.Gz

1. Introduction

For many years the III–V group nitride materials have attracted a lot of attention as candidates for the application in high voltage and high power electronic devices suitable to operate at high frequencies and high temperature [1, 2]. The AlGaN/GaN based terahertz (THz) emitters and detectors possessing a two-dimensional electron gas (2DEG) localised at the heterostructure interface have also been proposed [3, 4]. It has been shown that a relatively poor quality and low thermal conductivity of heterostructures grown on a sapphire substrate are the main obstacles that limit the efficiency of THz radiation from electrically driven 2DEG plasmons [3]. Although the first high-electron-mobility transistors (HEMTs) and Schottky diodes (SDs) have been demonstrated on the AlGaN/GaN grown on a native GaN substrate [5], its further development is limited by the high price and small volume production of the GaN crystals. Thus, to make progress in the GaN technology, AlGaN/GaN structures grown on foreign substrates such as silicon [6], sapphire [7], and SiC [8] have been explored. Usually the AlGaN/GaN structures with less demanding performance are fabricated on sapphire or silicon substrates. However, such devices suffer from a larger amount of defects and wafer bending caused by the mismatch of the lattice constant and the difference in the coefficient of thermal expansion [6, 9]. On the other hand, AlGaN/GaN HEMTs on a semi-insulating SiC (SI SiC) substrate exhibit a superior performance due to a smaller lattice mismatch and significantly higher thermal conductivity both of which are of vital importance for high power

applications [2]. In this work the AlGaN/GaN based SD and HEMT devices grown on a SI SiC substrate were developed. Electrical characteristics were measured and compared with similar heterostructure devices processed on a sapphire substrate. In addition, the suitability for detection of THz waves with the AlGaN/GaN HEMT on SI SiC at room temperature is demonstrated.

2. Device fabrication

AlGaN/GaN heterostructures were grown on a 500-μm-thick four-inch diameter SI 6H-SiC substrate by the metalorganic chemical vapour deposition (MOCVD) method at the Institute of High Pressure Physics (UNIPRESS), Poland. The growth procedure began with UNIPRESS proprietary nucleation epilayers followed by 1-μm-thick unintentionally doped (UID) GaN and 19-nm-thick $Al_xGa_{1-x}N$ (x = 0.25) layers with a 1-nm-thick AlN spacer in between. The schematic view of the structure is shown in Fig. 1(a). An electrical conductance is provided by the 2DEG channel which is localized nearby AlN spacer in the top part of the GaN layer. Both the thickness of the AlGaN barrier and the Al molar fraction x in the $Al_xGa_{1-x}N$ layer were determined from the X-ray diffraction measurements. Finally, the heterostructure was *in situ* covered by a 2-nm-thick GaN cap and a 1-nm-thick SiN layer. The measurements of a contactless nondestructive sheet resistivity and Hg-probe free-carrier density provided the values of 397±5 Ω/□ and 3.6 × 10^{12} cm^{-3} at room temperature, respectively. The root mean square (RMS) value of the surface roughness, estimated from the images of atomic force microscopy, was of about 0.44 nm.

The samples were processed at the Center for Physical Sciences and Technology (FTMC), Lithuania. Standard ultraviolet (UV) photolithography was used to provide the geometry of devices. The Ti/Al/Ni/Au (30/90/20/100 nm) ohmic contacts deposited by e-beam thin-film metal deposition were annealed by rapid thermal annealing (RTA) [7]. The Schottky contacts were eventually formed of Ni/Au (25/200 nm) metal stack. The mesa etching procedure was not involved in order to minimize the fabrication steps. The circular transmission line method was used to evaluate the performance of ohmic contacts [10]. Values for the contact resistance R_c and specific contact resistivity ρ_c were minimized down to 1 Ω mm and 2 × 10^{-5} Ω cm^2, respectively.

3. Results and discussion

3.1. Schottky diodes (SDs)

Several sets of planar SDs were developed with a circular Schottky contact with the radius of L = 40 μm in the centre. The distance d between the inner Schottky and outer ohmic electrodes was varying from 5 to 40 μm with a step of 5 μm. The current–voltage (I–V) characteristics were measured by applying a DC bias in the range from −210 to +2 V, and the results are shown in Fig. 2. The leakage current of the SDs with d = 40 μm saturates at a value of 3.3±1.1 mA/cm^2. The latter value is more than one order of magnitude smaller in comparison to the SDs of a similar design processed on the sapphire substrate [7]. In the regime of forward voltage the maximum current density reaches the value up to 94±12 A/cm^2.

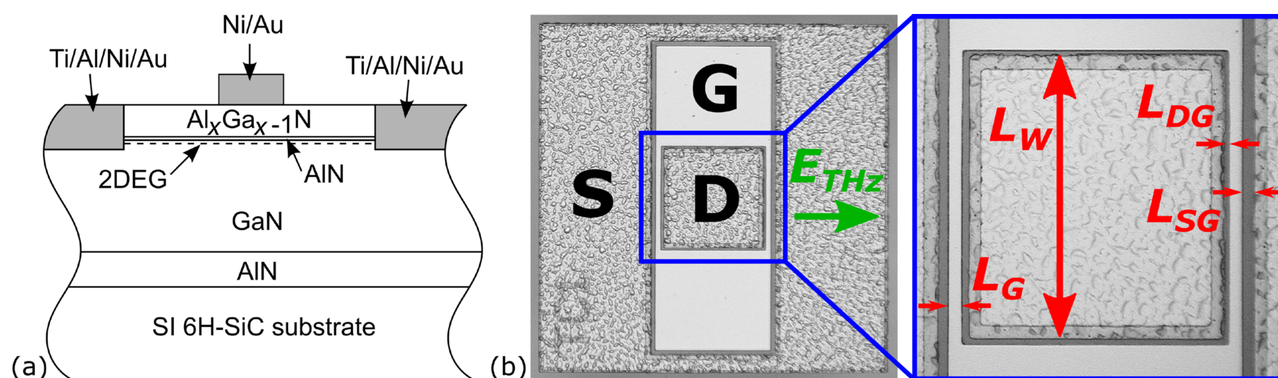

Fig. 1. (a) Schematic cross-section of the AlGaN/GaN/SiC heterostructure with processed electric contacts. Picture (b) presents the microscope image of the AlGaN/GaN HEMT.

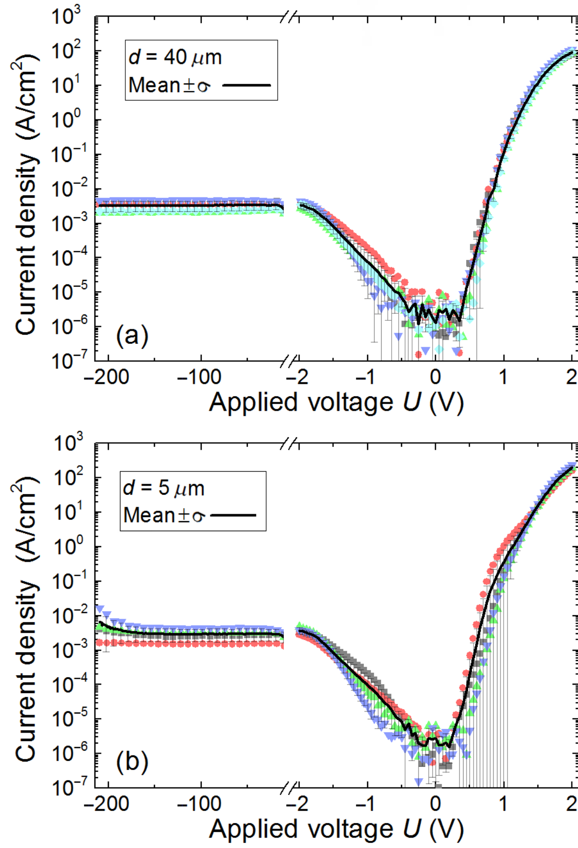

Fig. 2. *I–V* characteristics of the Schottky diodes with (a) d = 40 μm and (b) d = 5 μm. The black line is the average value and the error bars indicate the value of one standard deviation. The current I was normalised to the area of the Schottky electrode $S = 5.027 \times 10^{-5}$ cm^2.

It should be noted that the saturation of the SDs was not observed at +2 V bias showing a possibility for further device improvement. Narrowing of the length of the 2DEG channel was realized in the SDs with d = 5 μm, and the results are shown in Fig. 2(b). Actually these diodes demonstrated up to two times larger forward current density, i.e. 200±30 A/cm², in comparison with the previous group of SDs. Moreover, the change of leakage current is insignificant and its value stays at the level of 3.0±1.2 mA/cm² under the reverse bias down to −170 V. Note that the ON–OFF ratio of electric current switching (I_{ON}/I_{OFF}) is above 50 dB within the entire voltage range. It should also be noted that the growth of leakage current dispersion increases with the reverse bias for the SDs with d = 5 μm, most probably due to the activation of emission centres at the interface. In spite of that, the measured leakage current density does not exceed a value of 10 mA/cm². In addition, the processed SDs were exposed under the reverse bias up to −210 V without a failure representing the range of the breakdown fields being larger than 420 kV/cm.

Figure 3 shows the SD capacitance–voltage (*C–V*) characteristics measured in the range from −7 V to 0 V. The threshold voltage (U_{th}) indicates a reverse bias needed to fully deplete the conductive 2DEG channel. In our experiments the value of U_{th} = −2.2 V was found to be independent

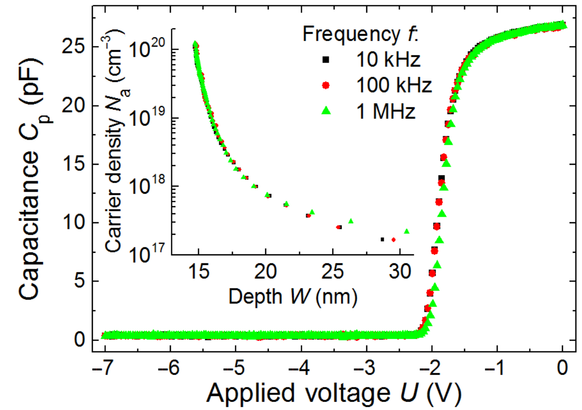

Fig. 3. *C–V* performance of the d = 40 μm SDs at selected modulation frequency. Inset: charge distribution along the AlGaN/GaN interface found from the *C–V* characteristic using Eqs. (2) and (3).

of the modulation frequency. The 2DEG density (N_{2DEG}) was evaluated using the integral capacitance technique described by [10]

$$N_{2DEG} = \frac{1}{eS} \int_{U_{th}}^{0} C_P(U)\,dU. \tag{1}$$

Here e is the electron charge and $C_P(U)$ is the capacitance measured by applying the reverse voltage. Integration of the *C–V* curve revealed that the 2DEG density was 5.9×10^{12} cm^{-2} with an uncertainty less than 2%. The dependence of carrier density on the depth is presented in the inset of Fig. 3. The depth W and carrier density N_a were calculated at each and all points of the measured *C–V* characteristic as follows [10]:

$$W = \frac{\varepsilon\varepsilon_0 S}{C_P}, \tag{2}$$

$$N_a = \frac{C_P^3}{e\varepsilon\varepsilon_0 S^2\, dC_P(U)/dU}. \tag{3}$$

Here $\varepsilon = 8.9$ is the relative permittivity of GaN, ε_0 is the electric constant, and $dC_p(U)/dU$ is the first order derivative of $C_p(U)$. The position of the 2DEG was found to be at 15 nm from the surface and is in agreement with the barrier thickness determined from the X-ray diffraction measurement. The values of the 2DEG density and the electron mobility, 8.3×10^{12} cm^{-2} and 1.9×10^3 cm^2/Vs at room temperature, and 6.9×10^{12} cm^{-2} and 17×10^3 cm^2/Vs at liquid nitrogen temperature, respectively, were provided from the Hall effect measurements. Note that the 2DEG density obtained from the Hall experiment is about 1.4 times larger as compared with the value calculated from the *C–V* measurements indicating ungated and gated 2DEG plasma peculiarities in the processed AlGaN/GaN heterostructures [3].

3.2. High-electron-mobility transistors (HEMTs)

The design of the HEMT is shown in Fig. 1(b). The HEMT consists of a rectangular drain in the centre surrounded with a ring-shape double gate and with a ring-shape source electrode. The size of the gate is $L_G \times L_W = 5.5 \times 100$ μm with a spacing between the source-drain and drain-gate of $L_{SD} = 11.5$ μm and $L_{DG} = 2.0$ μm, respectively. Typical HEMT DC-output characteristics are shown in Fig. 4(a). The drain saturation current and the ON-state resistance (R_{ON}) are 450 mA/mm and 40 Ω, respectively. The actual R_{ON} is smaller if one takes into consideration the contact resistance providing an estimated value of $R_{ON} = 28$ Ω. It is also worth noting that there is almost no decrease of current in the high U_{DS} region showing more efficient Joule heat dissipation due to the 10 times higher thermal conductivity of the SiC as compared to that of the sapphire.

The DC transfer characteristics are shown in Fig. 4(b). The threshold voltage around –2.2 V is consistent with the value obtained from the *C–V* measurements (see Fig. 3). The leakage currents demonstrate a weak dependence on the source-drain voltage while the absolute values are several orders of magnitude smaller as compared with the HEMT processed on the sapphire [7]. In this work HEMTs with an improved performance exhibit values of the ON–OFF ratio up to $I_{ON}/I_{OFF} = 70$ dB and the transconductance up to $g_m = 165$ mS/mm at $U_{DS} = 2$ V and $U_{GS} = 0$ V.

3.3. Detection of THz waves with HEMT

The detection of the THz frequency electromagnetic waves is demonstrated employing the HEMT as a TeraFET detector [11]. A commercial *VDI* electronic frequency multiplier chain emitting up to 11 mW power at 0.3 THz frequency was used as the source. The emission power was electrically modulated at 1 kHz frequency and detected with the HEMT using the lock-in amplifier technique. The orientation of the THz

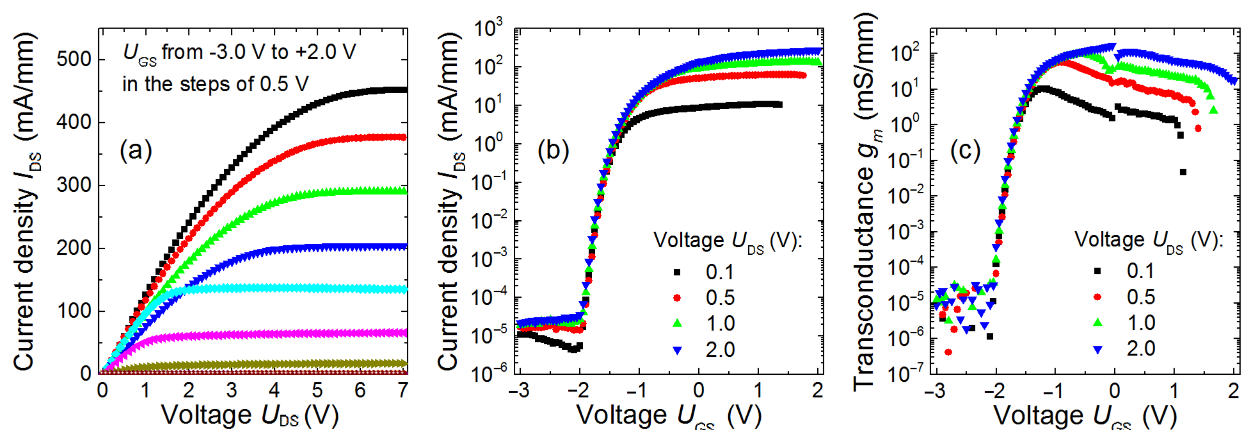

Fig. 4. Measured DC characteristics of the HEMT device: (a) output at the gate voltage from –3.0 to 2.0 V in steps of 0.5 V (note that curves below $U_{GS} = -1.5$ V overlap), (b) transfer and (c) transconductance at selected drain voltages. The current I_{DS} in (a) and (b) figures was normalised to the double width of HEMT gate, $2L_W = 200$ μm.

electric field with respect to the HEMT electrodes is shown in Fig. 1(b). The THz beam was focused on the HEMT from the substrate side using a 2-inch-diameter 1/#2 off-axis parabolic mirror and an aplanatic silicon lens. The HEMT was connected in a common-source mode circuit, positioned on a translation stage, and raster scanned in the focal plane of the focused THz beam. The results are presented in Fig. 5. The total optical responsivity *R* and the noise equivalent power (*NEP*) were estimated. In the case of U_{GS} = 0 V, the HEMT demonstrated the values of *R* = 30 mV/W and *NEP* = 26 nW/√Hz, while at U_{GS} = –1.5 V, these values were 90 mV/W and 107 nW/√Hz, respectively. Such THz wave detection using the SiC-based AlGaN/GaN HEMT is demonstrated for the first time. In the future work, the responsivity and *NEP* values can be optimized by proper THz antenna connection [12] and by reduction of the plasmonic channel measurements [11].

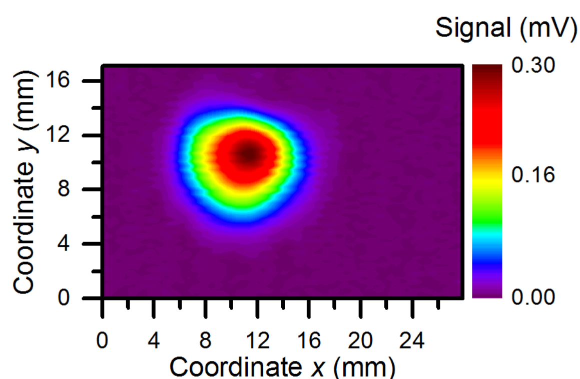

Fig. 5. Beam profile of the 300 GHz frequency source measured using the AlGaN/GaN HEMT biased at U_{GS} = 0 V. Pixel size is 0.3 × 0.3 mm^2.

4. Conclusions

In conclusion, the electronic devices, namely SDs and HEMTs, have been developed from the AlGaN/GaN on the semi-insulating SiC substrate. All devices demonstrated a significant improvement of the performance in comparison with the SDs and HEMTs processed on the sapphire substrate. The fabricated devices exhibited much smaller leakage current densities and a higher I_{ON}/I_{OFF} ratio with the values down to 3.0±1.2 mA/cm^2 and up to 70 dB under the reverse electric field down to 340 kV/cm, respectively. The increase of steady currents and transconductance, as well as the thermal management of the HEMTs were mainly explained by the higher 2DEG mobility and higher thermal conductivity of the SiC substrate. We propose that a more effective heatsink will help in reducing the amount of the black-body radiation from the electrically driven large-area plasmonic THz emitters. Finally, the first successful THz detection experiment using the AlGaN/GaN HEMT as a TeraFET detector was demonstrated opening further routes for the optimization of THz designs. These achievements encourage the creation of novel plasmonic THz devices in the future.

Acknowledgements

The support from the Research Council of Lithuania (Grant No. LAT 04/2016) is acknowledged.

References

[1] R.S. Pengelly, S.M. Wood, J.W. Milligan, S.T. Sheppard, and W.L. Pribble, A review of GaN on SiC high electron-mobility power transistors and MMICs, IEEE Trans. Microw. Theory Tech. **60**(6), 1764–1783 (2012), https://doi.org/10.1109/TMTT.2012.2187535

[2] R. Quay, *Gallium Nitride Electronics* (Springer Berlin Heidelberg, Berlin, Heidelberg, 2008), https://doi.org/10.1007/978-3-540-71892-5

[3] V. Jakštas, I. Grigelionis, V. Janonis, G. Valušis, I. Kašalynas, G. Seniutinas, S. Juodkazis, P. Prystawko, and M. Leszczyński, Electrically driven terahertz radiation of 2DEG plasmons in AlGaN/GaN structures at 110 K temperature, Appl. Phys. Lett. **110**(20), 202101 (2017), https://doi.org/10.1063/1.4983286

[4] S. Boppel, M. Ragauskas, A. Hajo, M. Bauer, A. Lisauskas, S. Chevtchenko, A. Rämer, I. Kasalynas, G. Valusis, H.-J. Würfl, et al., 0.25-μm GaN TeraFETs optimized as THz power detectors and intensity-gradient sensors, IEEE Trans. Terahertz Sci. Technol. **6**(2), 348–350 (2016), https://doi.org/10.1109/TTHZ.2016.2520202

[5] P. Kruszewski, P. Prystawko, I. Kasalynas, A. Nowakowska-Siwinska, M. Krysko, J. Plesiewicz,

J. Smalc-Koziorowska, R. Dwilinski, M. Zajac, R. Kucharski, and M. Leszczynski, AlGaN/GaN HEMT structures on ammono bulk GaN substrate, Semicond. Sci. Technol. **29**(7), 75004 (2014), https://doi.org/10.1088/0268-1242/29/7/075004

[6] D. Zhu, D.J. Wallis, and C.J. Humphreys, Prospects of III-nitride optoelectronics grown on Si, Rep. Prog. Phys. **76**(10), 106501 (2013), https://doi.org/10.1088/0034-4885/76/10/106501

[7] V. Jakštas, I. Kašalynas, I. Šimkienė, V. Strazdienė, P. Prystawko, and M. Leszczynski, Schottky diodes and high electron mobility transistors of 2DEG AlGaN/GaN structures on sapphire substrate, Lith. J. Phys. **54**(4), 227–232 (2014), https://doi.org/10.3952/physics.v54i4.3011

[8] P. Kruszewski, M. Grabowski, P. Prystawko, A. Nowakowska-Siwinska, M. Sarzynski, and M. Leszczynski, Properties of AlGaN/GaN Ni/Au-Schottky diodes on 2°-off silicon carbide substrates, Phys. Status Solidi **214**(4), 1600376 (2017), https://doi.org/10.1002/pssa.201600376

[9] Y. Cordier, N. Baron, F. Semond, J. Massies, M. Binetti, B. Henninger, M. Besendahl, and T. Zettler, *In situ* measurements of wafer bending curvature during growth of group-III-nitride layers on silicon by molecular beam epitaxy, J. Cryst. Growth **301–302**, 71–74 (2007), https://doi.org/10.1016/j.jcrysgro.2006.11.126

[10] D.K. Schroder, *Semiconductor Material and Device Characterization*, 3rd ed. (John Wiley & Sons, Inc., Hoboken, NJ, USA, 2005), https://doi.org/10.1002/0471749095

[11] M. Bauer, R. Venckevičius, I. Kašalynas, S. Boppel, M. Mundt, L. Minkevičius, A. Lisauskas, G. Valušis, V. Krozer, and H.G. Roskos, Antenna-coupled field-effect transistors for multi-spectral terahertz imaging up to 4.25 THz, Opt. Express **22**(16), 19235 (2014), https://doi.org/10.1364/OE.22.019235

[12] A. Sešek, I. Kašalynas, A. Žemva, and J. Trontelj, Antenna-coupled Ti-microbolometers for high-sensitivity terahertz imaging, Sens. Actuators A Phys. **268**, 133–140 (2017), https://doi.org/10.1016/j.sna.2017.11.029

AlGaN/GaN/SiC DIDELIO ELEKTRONŲ JUDRIO TRANZISTORIŲ THz DETEKCIJAI SUKŪRIMAS

V. Jakštas [a], J. Jorudas [a], V. Janonis [a], L. Minkevičius [a], I. Kašalynas [a], P. Prystawko [b], M. Leszczyński [b]

[a] *Fizinių ir technologijos mokslų centras, Vilnius, Lietuva*

[b] *Aukštų slėgių fizikos institutas UNIPRESS, Varšuva, Lenkija*

Santrauka

Darbe pristatomi Šotkio diodai ir didelio elektronų judrio tranzistoriai (HEMT), sukurti AlGaN/GaN heterodarinių, užaugintų ant pusiau izoliuojančio SiC padėklo, pagrindu. Šie elektroniniai įtaisai pasižymi geresniais elektriniais parametrais, palyginti su analogiškais įtaisais, pagamintais iš ant safyro padėklo užaugintų heterostruktūrų. Tiek Šotkio diodai, tiek HEMT išsiskyrė mažesnėmis nuotėkio srovėmis ir didesniu srovių I_{ON}/I_{OFF} santykiu, kurių skaitinės vertės atitinkamai neviršijo 3,0±1,2 mA/cm^2 ir siekė iki 70 dB, kai užtvarine kryptimi pridedamas iki 340 kV/cm stiprio elektrinis laukas. Be to, buvo išmatuotos didesnės HEMT kanalu tekančios srovės, kurios pasižymėjo stabilumu, ir pereigos laidžio vertės. Visas šias pagerėjusias elektrines savybes lemia efektyvesnis šilumos atidavimas iš įtaisų aktyviosios srities į aplinką, o tam turi įtakos didesnis SiC šiluminio laidumo koeficientas. Parodyta, kad AlGaN/GaN HEMT geba registruoti THz dažnio spinduliuotę kambario temperatūroje, o detektorių charakterizuojančius parametrus būtų galima optimizuoti parenkant tinkamą THz anteną bei detektoriaus matmenis. Šie rezultatai atveria galimybes ieškoti tinkamiausių sprendimų kuriant naujoviškus plazmoninius THz prietaisus Lietuvoje.